Density functional theory-based simulations of sum frequency generation spectra involving methyl stretching vibrations: effect of the molecular model on the deduced molecular orientation and comparison with an analytical approach

F Cecchet[1], D Lis[1], Y Caudano[1], A A Mani[1,4], A Peremans[1], B Champagne[2] and J Guthmuller[3]

[1] Research Centre in Physics of Matter and Radiation (PMR), FUNDP-University of Namur, 61 rue de Bruxelles, B-5000 Namur, Belgium
[2] Laboratory of Theoretical Chemistry (LCT), FUNDP-University of Namur, 61 rue de Bruxelles, B-5000 Namur, Belgium
[3] Faculty of Applied Physics and Mathematics, Gdansk University of Technology, Narutowicza 11/12, 80233, Gdansk, Poland

E-mail: francesca.cecchet@fundp.ac.be

Abstract

The knowledge of the first hyperpolarizability tensor elements of molecular groups is crucial for a quantitative interpretation of the sum frequency generation (SFG) activity of thin organic films at interfaces. Here, the SFG response of the terminal methyl group of a dodecanethiol (DDT) monolayer has been interpreted on the basis of calculations performed at the density functional theory (DFT) level of approximation. In particular, DFT calculations have been carried out on three classes of models for the aliphatic chains. The first class of models consists of aliphatic chains, containing from 3 to 12 carbon atoms, in which only one methyl group can freely vibrate, while the rest of the chain is frozen by a strong overweight of its C and H atoms. This enables us to localize the probed vibrational modes on the methyl group. In the second class, only one methyl group is frozen, while the entire remaining chain is allowed to vibrate. This enables us to analyse the influence of the aliphatic chain on the methyl stretching vibrations. Finally, the dodecanethiol (DDT) molecule is considered, for which the effects of two dielectrics, i.e. n-hexane and n-dodecane, are investigated. Moreover, DDT calculations are also carried out by using different exchange–correlation (XC) functionals in order to assess the DFT approximations. Using the DFT IR vectors and Raman tensors, the SFG spectrum of DDT has been simulated and the orientation of the methyl group has then been deduced and compared with that obtained using an analytical approach based on a bond additivity model. This analysis shows that when using DFT molecular properties, the predicted orientation of the terminal methyl group tends to converge as a function of the alkyl chain length and that the effects of the chain as well as of the dielectric environment are small. Instead, a more significant difference is observed when comparing the DFT-based results with those obtained from the analytical approach, thus indicating the importance of a quantum chemical description of the hyperpolarizability tensor elements of the methyl group.

1. Introduction

Vibrational optical techniques, such as infrared (IR) spectroscopy and Raman spectroscopy, are extensively used to probe the structural characteristics of thin organic layers at interfaces [1–4]. In the last 20 years, vibrational sum frequency generation (SFG) spectroscopy has become a reference tool to explore the structure and the organization of molecular films, thanks to its high surface sensitivity and to its strict selection rules, which have led to a deep understanding of the molecular structure at any kind of interface, either solid, liquid or gaseous [5–7]. While IR and Raman spectroscopies are based on linear optical phenomena, SFG spectroscopy involves a second-order nonlinear optical process. Within the harmonic approximation, IR absorption occurs when the electric field of the incident radiation, tuned in the IR frequency region, resonates with a molecular vibrational frequency, its intensity depending on the variation of the electric dipole moment along the normal coordinate. The Raman effect occurs when a radiation, often in the visible range, undergoes an inelastic process with a molecule, a substrate or both: a photon is generated at a frequency lower or higher than the incident radiation, the frequency shift corresponding to the frequency difference between the initial and final vibrational states. Neglecting anharmonicity effects, the Raman scattering intensity is related to the changes of molecular polarizability along the vibrational modes.

In SFG spectroscopy two coherent laser beams, one fixed in the visible range (ω_{vis}) and one tunable in the IR frequency region (ω_{IR}), overlap spatially and temporally and induce a nonlinear polarization. From the second-order nonlinear susceptibility contribution of the material (χ^2)—or, at the molecular level, from the first hyperpolarizability (β)—a third radiation at the sum of the incident frequencies $\omega_{\mathrm{SFG}} = \omega_{\mathrm{vis}} + \omega_{\mathrm{IR}}$ is generated. Since, in the dipole approximation, the second-order responses vanish for centro-symmetric systems, and therefore for many molecules and bulk materials, SFG spectroscopy is well suited for the investigation of interfaces, like the organic molecular films investigated in this contribution, where the inversion symmetry is broken. When scanning over the IR frequency, the SFG signal is enhanced when ω_{IR} resonates with a vibrational frequency of the interface, hence displaying its vibrational fingerprint. The vibrational mode has to be both IR and Raman active in order to be SFG active. At the molecular level, the interpretation of the SFG response of the interface is done from the analysis of the IR dipole moment vector and of the Raman polarizability tensor, which both define the first hyperpolarizability. At the macroscopic or interface level, the orientation of the first hyperpolarizability of each molecule contributes to the macroscopic susceptibility tensor, which holds the average orientational information of the molecular films with respect to the interface.

A fundamental point when analysing the molecular orientation from SFG data is certainly the knowledge of the nonlinear susceptibilities associated to the measured vibrations. Indeed, though SFG is a very powerful tool, straightforward interpretations of the spectra are often hampered by the difficulty to precisely quantify the IR vectors and Raman tensors, which define the molecular first hyperpolarizability, and consequently the second-order susceptibility of the interface. One possible approach to get more quantitative and reliable information about the molecular orientation consists in combining SFG measurements with a theoretical analysis. Since the earlier works [8–11], the orientation analyses have mainly focused on the SFG signature of the ubiquitous methyl group employing an analytical representation of its nonlinear susceptibility, which is based on a bond additivity model (BAM) for both the dipole moment and polarizability derivatives. Following that, as reviewed in [12], several theoretical works have been devoted to refining the analytical modelling of the CH_3 susceptibility. Later, it has also been shown that the orientation of adsorbed molecules at interfaces or the structure of water surfaces can be addressed by performing dedicated simulations and subsequent interpretations of the experimental vibrational SFG spectra [13, 14]. These methods encompass, on the one hand, static approaches generally based on first principles calculations for describing the SFG responses of molecules, supramolecules, and aggregates in well-defined configurations and, on the other hand, molecular dynamics (MD) simulations based on molecular mechanics or first principles methods to account for the numerous structural configurations of the interfaces. The integration of MD aspects into the simulation of vibrational SFG spectra has recently been reviewed by Morita and Ishiyama [15] while related approaches are also employed for the IR spectra of gas and liquid phases [16]. As a function of the nature of the interfaces, these two classes of computational tools have a distinct impact: for example, MD is necessary when studying liquid surfaces, like gas–water interfaces, whereas the other methods are well adapted for determining the SFG signatures of interfacial organic films [17, 18].

In this paper, we focus on the vibrational signatures of the terminal methyl group of alkanethiol monolayers on Pt surfaces by using molecular responses evaluated at the density functional theory (DFT) level of approximation. This enables us to extend the existing models by accounting for the surroundings of the methyl groups. Here, the surroundings encompass both the chemical environment of the methyl group, i.e. the remaining part of the alkanethiol, and the other molecules as well as the solvent, which are represented by a dielectric. This study is carried out by analysing first the vibrational IR and Raman activities of the CH_3 stretching vibrations and then by simulating the SFG spectra, which are used to retrieve the orientation of the CH_3 group in the monolayer (the tilt angle) from comparison with the experimental spectra. With this aim, DFT calculations are carried out on three types of molecular models (figure 1). The first type consists in aliphatic chains, containing from 3 to 12 carbon atoms, in which only one methyl group can freely vibrate, while the rest of the chain is frozen by a strong overweight of its C and H atoms ($\sim$1000$\times$). This enables us to localize the probed vibrational modes on the methyl group, similarly to what is obtained by the analytical approach. In the second class, only one methyl group is frozen, while the
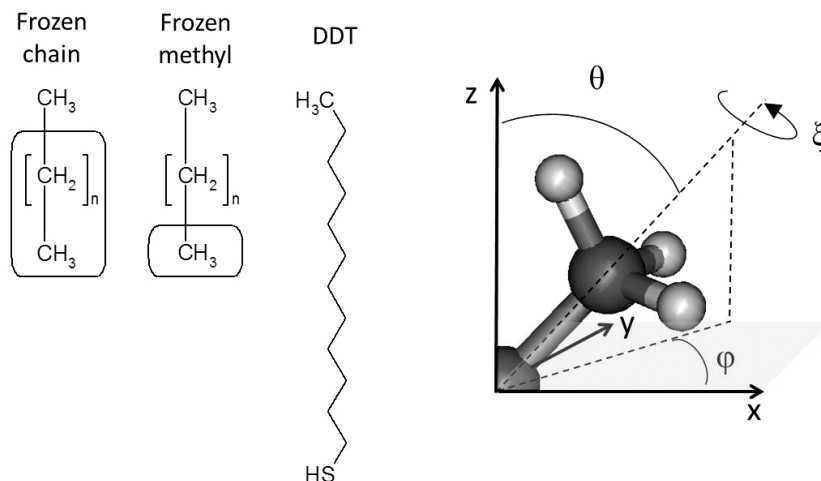
Figure 1. Left: schematic representation of the molecular models 'frozen chain', 'frozen methyl' and the DDT molecule. Right: definition of the three Euler angles.

entire remaining chain is allowed to vibrate. This enables a deeper analysis of the effect of the aliphatic chain on the methyl stretching vibrations. Finally, the dodecanethiol (DDT) molecule is considered, in which the effects of two dielectrics, i.e. n-hexane and n-dodecane, are investigated. Moreover, DDT calculations are also carried out by using different exchange–correlation (XC) functionals in order to investigate the DFT approximations.

2. Methodologies

2.1. Theoretical background

Though the general theory of surface SFG has already been reviewed [19–21], a short description of the main assumptions and equations is given below in order to outline the procedure used to calculate the SFG intensities. The SFG intensity I^{SFG} reads

$$I^{\text{SFG}} \propto |\chi^{(2)\text{NR}} + \chi^{(2)\text{R}}|^2 \quad (1)$$

where $\chi^{(2)\text{NR}}$ and $\chi^{(2)\text{R}}$ represent the non-resonant and resonant contributions to the effective susceptibility. Usually, most of the non-resonant part originates from the substrate while the resonant signatures come from the adsorbate vibrations. Within the harmonic approximation, the expression of the components of the rank 3 tensor of the resonant part is:

$$\chi_{ijk}^{(2)\text{R}} \propto \frac{\omega_{\text{SFG}}}{c} \frac{N_s}{\cos\theta_{\text{SFG}}} F^{\text{SFG},i} F^{\text{vis},j} F^{\text{IR},k}$$
$$\times \left\{ \sum_v \frac{1}{\omega_v} \frac{1}{(\omega_v - \omega_{\text{IR}} - i\Gamma_v)} \left\langle \sum_{l,m,n} T_{ijk}^{lmn} \frac{\partial\alpha_{lm}}{\partial Q_v} \frac{\partial\mu_n}{\partial Q_v} \right\rangle \right\} \quad (2)$$

$\partial\alpha_{lm}/\partial Q_v$ and $\partial\mu_n/\partial Q_v$ are the first derivatives of the polarizability and dipole moment with respect to the vth vibrational normal mode. T_{ijk}^{lmn} rotates the molecule to the surface coordinates system, the brackets represent an average over the orientation distribution of the ad-molecules, Γ_v is the

half width at half maximum of the assumed Lorentzian band shape, and N_s is the density of molecules on the surface. The Fresnel factors $F^{\text{SFG},i}$, $F^{\text{vis},j}$ and $F^{\text{IR},k}$ describe the amplitude of the components of the total electric field generated at the interface at the frequency of the three coherent laser beams.

The orientation of the molecule is defined by the Euler angles ϑ, ξ, φ (figure 1). We assume that (i) all molecules have the same tilt ϑ and rotation ξ angles; in other words, we consider a Dirac distribution for both ϑ and ξ angles, (ii) all the molecules are arranged in molecular domains over the surface, which result in an effective achiral and rotationally isotropic surface. This means that the surface is assumed invariant for arbitrary rotations around the surface normal (Z axis, φ angle) and for a mirror reflection from a plane perpendicular to the surface. These assumptions imply that only seven components of the susceptibility are non-zero and four of them are independent ($\chi_{ZZZ}^{(2)}$, $\chi_{XXZ}^{(2)} = \chi_{YYZ}^{(2)}$, $\chi_{XZX}^{(2)} = \chi_{YZY}^{(2)}$, $\chi_{ZXX}^{(2)} = \chi_{ZYY}^{(2)}$). These components are then computed from the molecular Raman tensors and IR vectors by performing an average over N molecules and a coordinate change from the molecular to the laboratory frame according to equation (2) [8–10].

2.2. Simulation approach

The SFG spectra of DDT have been simulated with a program developed in our laboratories according to equations (1) and (2). This program (i) makes use of the Raman tensors $\partial\alpha_{lm}/\partial Q_v$ and IR vectors $\partial\mu_n/\partial Q_v$ of each vibrational normal mode of the molecule, (ii) computes the Fresnel factors at the Pt/monolayer/air interface and (iii) takes into account the experimental geometry.

In the present simulations the non-resonant contribution (first term of equation (1)) is assumed to be zero. Indeed, although this term may become important, even dominant for some substrates such as gold, this is not the case for platinum [22], which does not possess any electronic transition close to the visible and/or SFG wavelengths. The

SFG intensity of the different vibrational modes is thus inferred directly from the experimental spectra without any non-resonant background subtraction. As stated above, the simulation of the spectra has been carried out by considering that all molecules have the same tilt and rotation angles. The use of this approximation is motivated by the fact that the substrate used in this work has a very low roughness (RMS = 0.2 nm), which facilitates the growth of directionally ordered monolayers. Moreover, with the purpose of comparing different theoretical approaches, the orientational analysis has been performed for a fixed value of the rotation angle equal to 60°. This value has been chosen according to the results of a previous work [18], in which both tilt and rotation angles have been unambiguously determined from an analysis of polarization-dependent SFG spectra in the *ppp* and *ssp* configurations (indicating the polarizations of SFG, Vis and IR beams, respectively). Thus, by using ξ equal to 60°, the experimental *ppp* spectrum has been simulated and the ϑ angle has been obtained by determining the value which best reproduces the peak intensity ratio between the asymmetric and the symmetric stretchings of the methyl group.

2.3. IR vectors and Raman tensors

First, the IR vectors and Raman tensors of the methyl stretchings have been obtained through an analytical approach considering the BAM, which is based on symmetry considerations of the CH_3 group as well as on the C–H bond polarizability and dipole moment derivatives [8–10, 12]. According to the measurements of Epple *et al* [23], a depolarization ratio of $r = 0.12$ has been used. This parameter strongly affects the relative peak intensities of the methyl stretchings and therefore the tilt angle value obtained from the analytical approach. This is a critical point since the measurement of the depolarization ratio from conventional Raman spectroscopy is not very accurate and can only be performed for gases or liquids. Other experimental approaches may provide a more accurate estimate of the depolarization ratio, such as photoacoustic Raman spectroscopy [24] or coherent anti-stokes Raman spectroscopy (CARS) [25].

Then, the molecular properties of the C_nH_{2n+2} ($n = 3–12$) aliphatic chains—hereafter labelled Cn—were obtained from DFT calculations with the B3LYP XC functional [26] and the $6\text{-}311{+}{+}G(d, p)$ basis set performed using the GAUSSIAN 03 program [27]. The ground state geometry of the molecular chains was optimized under the condition that residual forces are smaller than 10^{-5} au.

Thereafter, the harmonic vibrational frequencies and normal coordinates were determined analytically at the same level of theory. These calculations were performed by 'freezing' either one methyl group (frozen methyl) or by 'freezing' the whole chain (frozen chain) with the exception of the terminal CH_3 group (figure 1). As already mentioned, the 'freezing' process consists of setting large atomic masses, 1000 amu and 10000 amu for the hydrogen and carbon atoms, respectively. Moreover, these calculations also provided the derivatives of the dipole moment with

respect to the normal coordinates $\partial\mu_n/\partial Q_v$ (IR vectors). The Raman tensors $\partial\alpha_{lm}/\partial Q_v$ were computed by using a two-point numerical differentiation procedure, where the static polarizability tensors are calculated for distorted structures, resulting from the addition or subtraction of a finite displacement along the normal coordinates to the equilibrium geometry. For the DDT molecule the calculations were performed with the GAUSSIAN 09 program [28], which employs an analytical differentiation procedure to calculate the vibrational frequencies, IR vectors, and Raman tensors. In addition to B3LYP, the effects of several XC functionals, namely the modified B97 [29] functional of Hamprecht *et al* (B97-1) [30], the last version of the Heyd–Scuseria–Ernzerhof functional (HSE06) [31], the Minnesota functionals (M06 and M06-2X) [32] as well as a Coulomb-attenuating functional, (CAM-B3LYP) [33], were investigated with the same basis set. Finally, the influence of a non-polar environment on the properties of DDT was taken into account by the integral equation formalism of the polarizable continuum model (IEFPCM). Such calculations were achieved with the B3LYP XC functional in n-hexane ($\varepsilon = 1.8819$) and n-dodecane ($\varepsilon = 2.0060$).

2.4. Experimental details

Self-assembled monolayers (SAMs) of dodecanethiol were grown on Pt(111) single crystals. The latter, which are mechanically polished, were first cleaned in a freshly prepared piranha solution (98% H_2SO_4/30% H_2O_2 7:3 v/v) and subsequently rinsed with 18 MΩ cm water. Then, they were thoroughly annealed with an oxygen-enriched butane before being immediately immersed overnight in a 1 mM ethanolic solution of DDT. The modified surfaces were abundantly rinsed in pure absolute ethanol and dried under a stream of nitrogen prior to SFG investigation. DDT molecules, and absolute ethanol (spectroscopic grade) were purchased from Sigma-Aldrich and used as supplied.

The SFG setup is a homemade spectrometer with two optical parametric oscillators (OPOs) synchronously pumped by a single picosecond Nd:YAG laser. The IR OPO is built around a $LiNbO_3$ crystal for the generation of the 2700–3700 cm^{-1} IR frequencies, while the vis OPO is made around a β-barium borate (BBO) crystal. The measurements have been carried out in a nearly co-propagative configuration, with the IR and vis incident beams at 65° and 55° with respect to the sample surface normal. After spectral filtering by a double grating monochromator, the SFG signal is amplified by a photomultiplier tube and monitored by an oscilloscope. The visible wavelength was kept constant at 532 nm, while the IR frequency has been scanned between 2750 and 3050 cm^{-1}.

3. Results and discussions

3.1. SFG spectrum of DDT SAM on Pt(111): analytical interpretation

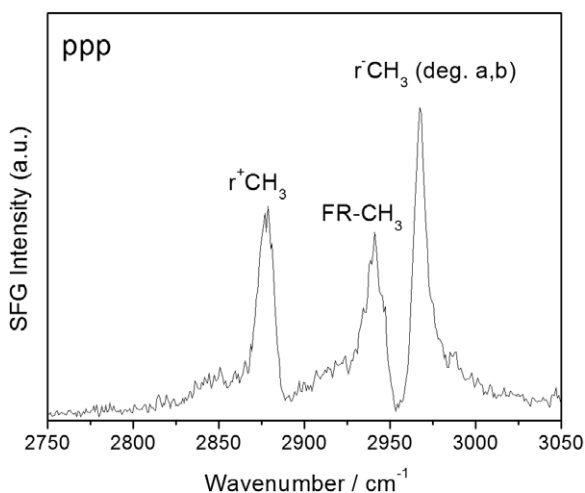The SFG spectrum of DDT SAM on Pt(111) (figure 2) recorded in the *ppp* polarization set shows three main

Figure 2. SFG spectrum of a DDT monolayer on platinum recorded with *ppp* set of polarizations. Reproduced with permission from [18]. Copyright 2010 John Wiley & Sons.

resonances that are assigned to CH_3 vibrations [18]: the doubly degenerate asymmetric stretchings (r^-CH_3, deg. *a* and deg. *b*) at 2965 cm^{-1}, the Fermi resonance (FR-CH_3) at 2940 cm^{-1}, and the symmetric stretching (r^+CH_3) at 2880 cm^{-1}. It is seen that the SFG spectrum shows an intensity ratio between the r^-CH_3 and r^+CH_3 peak area of 1.25, which is used to determine the tilt angle θ of the methyl axis. Indeed, assuming a fixed rotation angle ξ equal to 60° (see section 2.2), the experimental spectrum can only be reproduced for a unique value of the tilt angle. Hence, by employing the analytical IR vectors and Raman tensors estimated following the bond additivity model [12] (figure 3), a tilt angle equal to 33° is found. The purpose of the next sections is the comparison of this result with those obtained employing DFT calculations performed on increasingly complex model systems. This will provide information on how the deduced orientational parameter depends on the method employed to obtain the IR and Raman tensors.

3.2. DFT simulations for free terminal methyl and frozen chains

In this part, the results for the molecular models in which only one methyl group can freely vibrate are discussed. For this case, the calculations provide for each chain length identical normal coordinates, which are exclusively localized on the methyl group, and which are similar to those of the analytical approach of Hirose *et al* [8–10] and Wang *et al* [12]. Therefore, these results allow us to investigate how an increasing aliphatic chain modifies the electronic density in the vicinity of the free methyl group and, consequently, to see how these changes affect the amplitudes of the IR and Raman tensors of the three methyl vibrations.

Figure 4 displays the calculated normal coordinates, IR vectors and the Raman tensors of the three methyl vibrations for representative chain lengths. By going from C3 to C12, the IR vectors of the three stretching modes remain oriented along the same directions, showing only a weak angular deviation (e.g. about 2° for r^+CH_3) in comparison to the analytical results (figure 3). Nevertheless, larger differences are found for the IR vectors of the symmetric with respect to the asymmetric *a* and *b* stretching modes when comparing the DFT and analytical approaches. Indeed, while the ratios of the norms of the analytical IR vectors r^+CH_3/r^-CH_3*a* and r^+CH_3/r^-CH_3*b* are both close to 0.47, they amount to 0.93 in the C3 model. Moreover, the DFT Raman tensors also present noticeable differences to those of the analytical approach. For example, the r^+CH_3/r^-CH_3*a* and r^+CH_3/r^-CH_3*b* ratios of the average Raman tensors obtained with the analytical model are equal to 1.38, while those obtained from DFT calculations on the C3 model correspond to 1.18 and 1.14, respectively. This can be understood from the fact that the polarizability—and subsequently the Raman tensors—depends on the outer part of the electronic
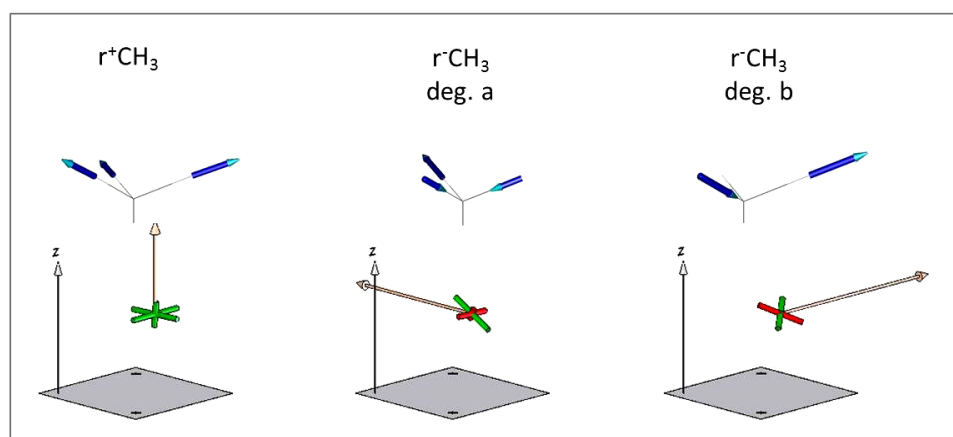

Figure 3. Sketch of the normal coordinates of the three methyl vibrational modes obtained from the analytical approach of Wang ([12]) with a depolarization ratio $r = 0, 12$ [23]. The IR vectors are shown in the molecular frame axis as pink arrows, while the Raman tensors are shown as green (red) rods for positive (negative) values. Reproduced with permission from [18]. Copyright 2010 John Wiley & Sons.
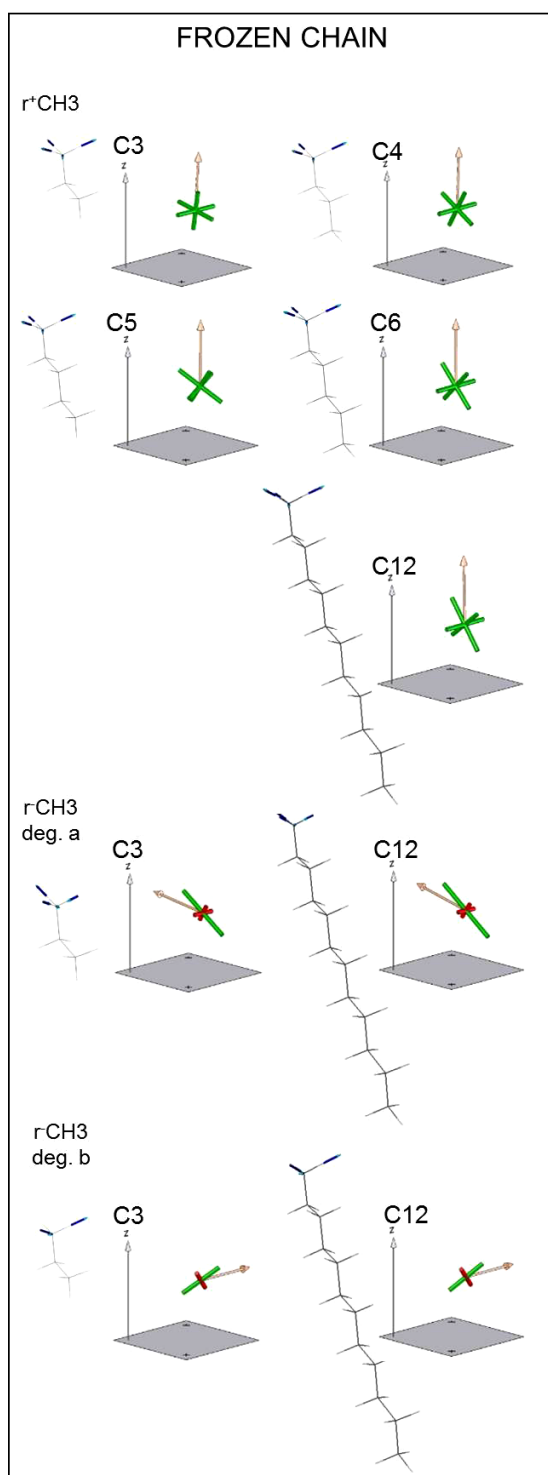
Figure 4. Sketch of the B3LYP normal coordinates of the three methyl modes of the 'frozen chain' models obtained with DFT calculations. The IR vectors are shown in the molecular frame axis as pink arrows, while the Raman tensors are shown as green (red) rods for positive (negative) values. The symmetric stretching mode is represented for the C3, C4, C5, C6 and C12 models, while the two degenerate asymmetric stretching modes are represented for the C3 and C12 models.

Figure 5. Evolution of the methyl tilt angle θ as a function of the number of carbon units in the molecular models, assuming a rotation angle ξ of 60°. (Top) 'frozen chain' and (bottom) 'frozen methyl' models.

density. Therefore, the Raman tensors are expected to be more influenced by the presence of the aliphatic chain than the IR ve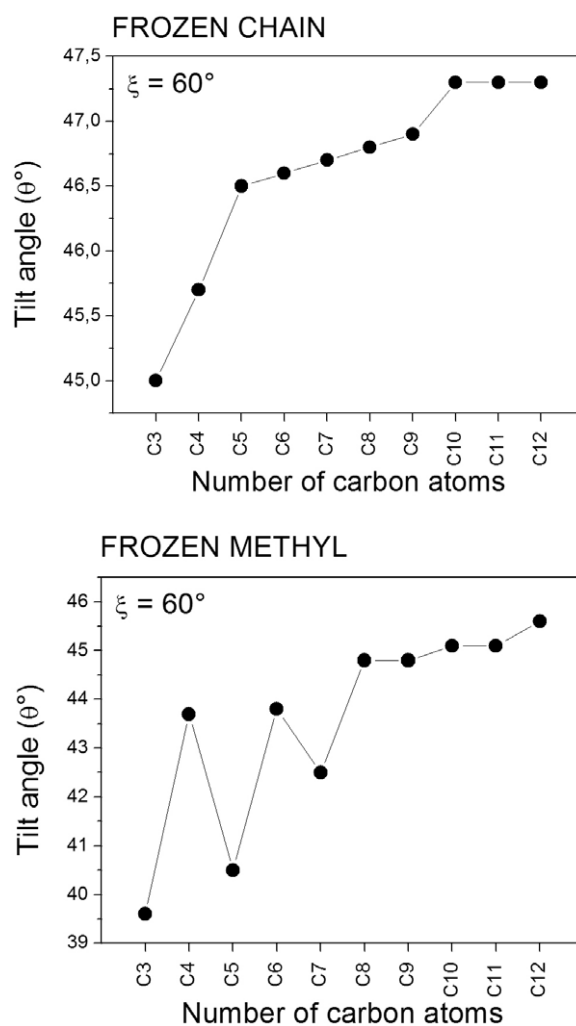ctors. Such an effect is clearly apparent for the Raman tensor of the symmetric stretching (r^+CH_3), which shows important variations going from the C3 to the C6 molecular models, while they are mostly identical in C6 and C12.

Figure 5 (top) displays the values of the tilt angles that allow reproducing the experimental SFG spectrum of DDT, i.e. the ratio of 1.25 between the intensities of the symmetric and asymmetric CH_3 stretching modes. The tilt angle shows an overall variation of about 2° going from the C3 (45.0°) to the C12 (47.3°) model but the largest change occurs between the C3, C4 and C5 models. This is related to the differences in the Raman tensors of the r^+CH_3 vibration. Then, for longer chains the tilt angle converges progressively to a value close to 47°. Therefore, it can be concluded that the effect of the aliphatic chain—considered as frozen—on the orientational parameter is rather modest. However, a significant difference is obtained in comparison to the analytical approach, which predicts a tilt angle of 33°. This deviation of about 14° can mostly be ascribed to the different relative intensities (IR and

Raman) obtained for the modes r^+CH_3 and r^-CH_3 when using the DFT or the parameters of the analytical approach.

3.3. DFT simulations for free chains and frozen terminal methyl

In this part, the model systems contain one methyl group that is kept frozen. These systems allow the investigation of changes in both the $\partial\mu_n/\partial Q_v$ and $\partial\alpha_{lm}/\partial Q_v$ quantities as well as changes of the methyl centred normal coordinates as a function of increasing chain length. Figure 6 shows the normal coordinates, IR vectors and Raman tensors obtained with the DFT calculations. First, it is seen that all three normal modes involve atomic motions on the CH_3 moiety but also on the two adjacent CH_2 units. This directly affects the values of the IR and Raman tensors, because these quantities are defined as derivatives of the dipole moment and the polarizability along the normal coordinates. Indeed, the IR vectors of the three vibrations show modifications in their orientations and norms in comparison to the 'frozen chain' models. For example, this is clearly visible in the case of the symmetric stretching (r^+CH_3), for which the IR vectors are tilted from the z-axis by about 13°, compared to the tilting of 2° observed for the 'frozen chain' models. Moreover, the r^+CH_3/r^-CH_3a and r^+CH_3/r^-CH_3b ratios for the C3 model correspond to 0.96 and 0.81, respectively, thus indicating large differences in the amplitude compared to the analytical model (0.47) as well as to a lesser extent to the computed 'frozen chain' model (0.93). Additionally, strong differences are obtained for the average Raman tensors, since the r^+CH_3/r^-CH_3a and r^+CH_3/r^-CH_3b ratios for the C3 model amount to 0.90 and 1.86, respectively, whereas they are equal to 1.38 for the analytical approach and to 1.18 and 1.14 for the C3 'frozen chain' system, respectively.

Similarly to the 'frozen chain' models, the Raman tensor of the r^+CH_3 vibration presents the largest variations when going from the C3 to the C6 molecular models. The values of the tilt angle obtained with the 'frozen methyl' data (figure 5, bottom) show an overall variation of about 6° going from the C3 (39.6°) to the C12 (45.6°) models. This value is somewhat larger than the one (about 2°) determined with the 'frozen chain' systems. Moreover, the values of the tilt angle display an oscillating behaviour for molecular system having odd or even numbers of carbon atoms. This effect is larger for short chains (C3 to C6) and decreases progressively for longer chains until the tilt angle converging towards 45° is reached. Hence, in the case of the C12 system almost similar tilt angles are found with a frozen chain (47.3°) and a frozen methyl (45.6°).

3.4. DFT simulations of DDT

In practical applications, the aliphatic chains are bonded to a metallic surface via a terminal thiol group. Therefore, in order to get closer to the experimental conditions, the IR and Raman tensors of the DDT molecule are investigated by assuming that all atoms can freely vibrate. The normal coordinates, IR vectors and Raman tensors of the methyl
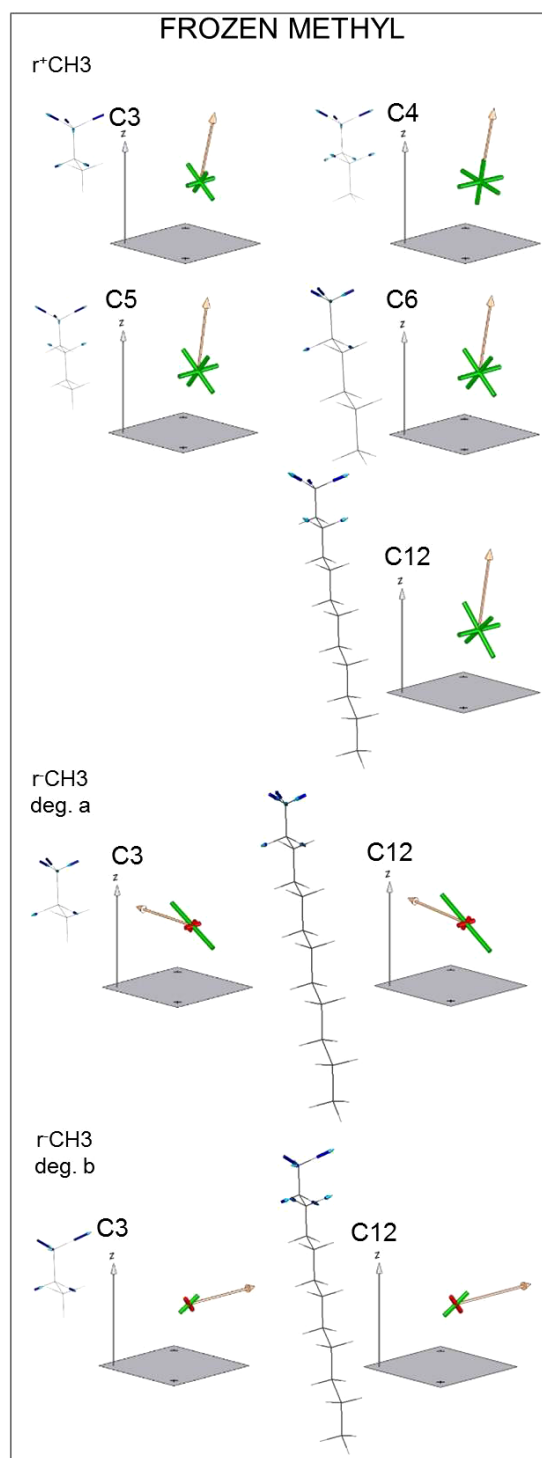

Figure 6. Representation of the normal coordinates of the three methyl modes of the 'frozen methyl' models obtained from B3LYP calculations. The IR vectors are shown in the molecular frame axis as pink arrows, while the Raman tensors are shown as green (red) rods for positive (negative) values. The symmetric stretching mode is represented for the C3, C4, C5, C6 and C12 models, while the two degenerate asymmetric stretching modes are represented for the C3 and C12 models.

vibrations are presented on top of figure 7. These data obtained with the B3LYP XC functional without accounting for surrounding effects match the results obtained for the C12
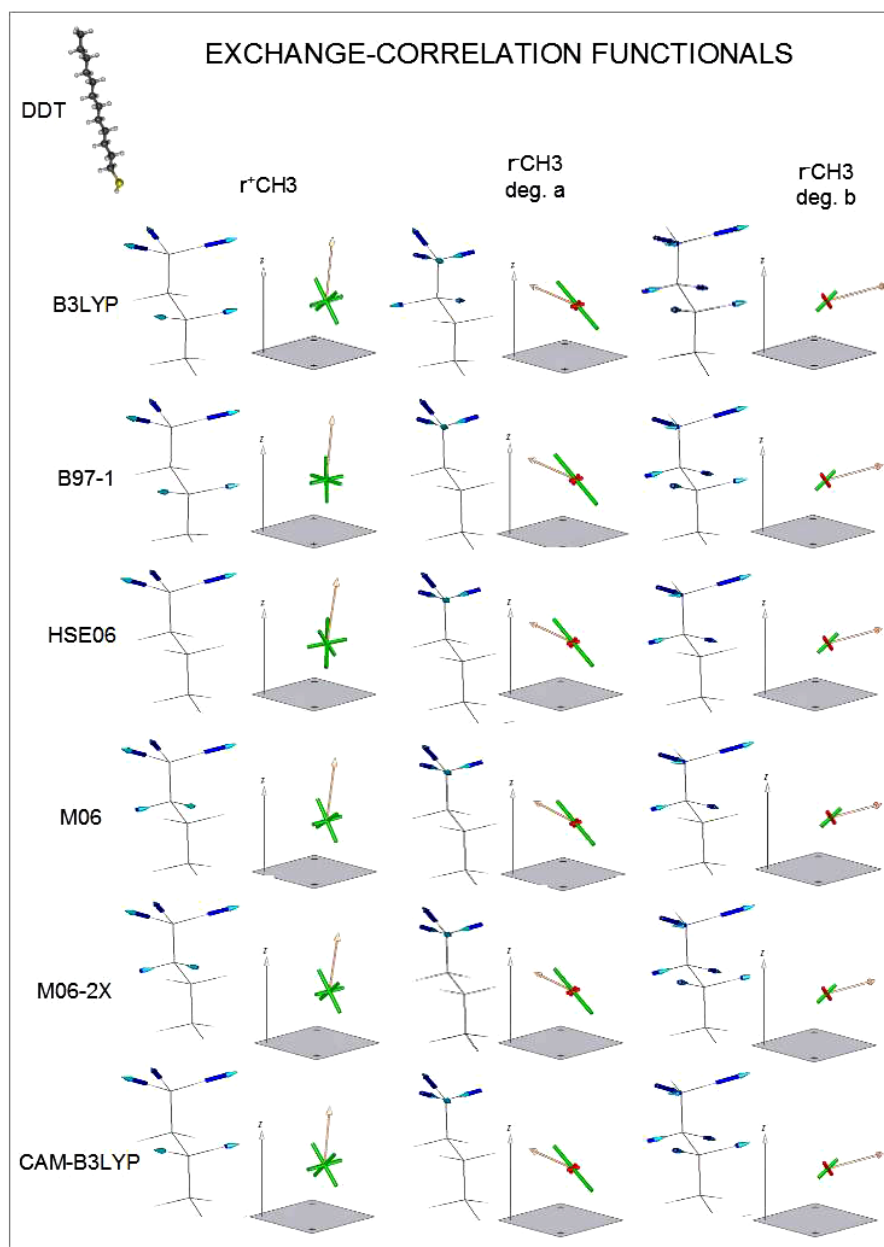
Figure 7. Representation of the calculated normal coordinates of the three methyl modes of the DDT model, obtained by using different exchange–correlation functionals. The IR vectors are shown in the molecular frame axis as pink arrows, while the Raman tensors are shown as green (red) rods for positive (negative) values.

system assuming a frozen methyl (figure 6). In particular, the normal modes of DDT display similar contributions from the methylene groups adjacent to the terminal methyl. A tilt angle of 43.4° is deduced for the DDT (figure 8), which deviates by about 2° in comparison to the C12 molecular model (45.6°).

In SAMs, intermolecular interactions are present between the molecular units and are therefore likely to influence the IR and Raman tensors. Herein, these interactions are investigated with the polarizable continuum model (PCM), which describes the effects of the environment in an average way. Since the surrounding is modelled by a dielectric (n-hexane and n-dodecane are simply represented by their dielectric constant), the specific molecular interactions are neglected. Under such conditions, the estimated tilt angle of the methyl group amounts to 44.0° and 44.1° in n-hexane and n-dodecane, respectively, in comparison to 43.4° in vacuum. Therefore, it is seen that environmental effects, as described by the PCM, are small for the DDT methyl vibrations. One also notices that the calculated vibrational frequencies of DDT decrease when going from vacuum to n-hexane and n-dodecane (table 1): this red shift is characteristic of the surrounding effects. However, it has only little consequence on the methyl orientation. It can also be mentioned that the calculated vibrational frequencies are in good agreement with experiment, showing deviations smaller than 15 cm^{-1}, which is the typically accuracy one can expect from DFT
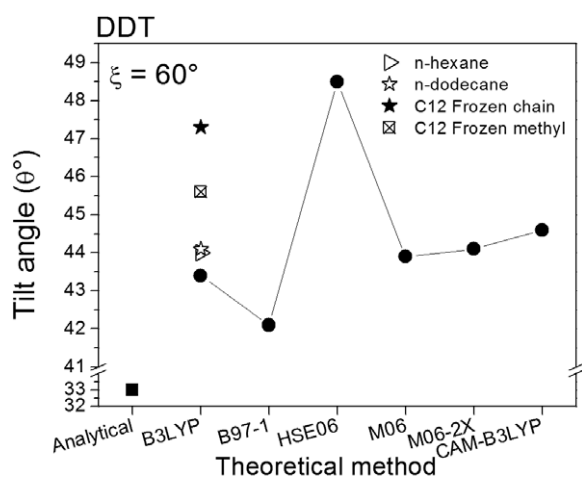
Figure 8. Black dots show the tilt angle of the methyl group as a function of the exchange–correlation functionals for the DDT model in vacuum, while the triangle and the empty star represent the values deduced for the DDT in n-hexane and n-dodecane. The black square accounts for the value obtained from the analytical approach. Other symbols summarize the values obtained for the C12 'frozen chain', and the C12 'frozen methyl'.

Table 1. Frequencies (cm^{-1}) of the symmetric and degenerate asymmetric stretchings of DDT as obtained from calculations in vacuum, in n-hexane and n-dodecane. (Note: frequencies have been scaled by a factor of 0.96.)

	Vacuum	n -hexane	n-dodecane
r^+CH_3	2896.0	2894.8	2894.7
r^-CH_3 (deg. a)	2953.9	2952.3	2952.1
r^-CH_3 (deg. b)	2958.1	2956.6	2956.5

calculations performed in the harmonic approximation after application of a scaling factor [34].

3.5. DFT simulations of DDT with different XC functionals

This section investigates how the choice of the computational method for calculating the IR and Raman tensors affects the deduced orientational parameters. Therefore, in addition to the B3LYP XC functional, DFT calculations of DDT have been carried out, still in vacuum, with five other XC functionals, namely B97-1, HSE06, M06, M06-2X, and CAM-B3LYP. The B3LYP, B97-1, HSE06, M06 and M06-2X are hybrid XC functionals having increasing amounts of Hartree–Fock (HF) exchange equal to 20%, 21%, 25%, 27% and 54%, respectively, whereas CAM-B3LYP is a long-range corrected XC functional. XC functionals with a moderate amount of HF exchange are usually well suited for the prediction of vibrational frequencies, whereas long-range corrected functionals or functionals having a larger amount of HF exchange were suggested to be more appropriate for the calculation of Raman intensities (see e.g. [35]). The normal modes, IR vectors and Raman tensors are reported in figure 7. For the symmetric stretching (r^+CH_3), the largest differences concern the Raman tensor obtained with the HSE06 XC functional and to a lesser extent the one calculated with

B97-1. The IR and Raman tensors obtained with the other XC functionals present more similarities. Some differences also concern the normal modes, which display variable contributions of the methylene units localized next to the methyl group.

The quantitative analysis of the experimental SFG spectrum obtained with these data indicates that the tilt angles fluctuate between 42.1° (B97-1) and 48.5° (HSE06) depending on the choice of the XC functional (figure 8). It can be noted that the tilt angle obtained with the HSE06 functional is significantly different from those deduced with the other XC functionals. Thus, besides the HSE06 functional, changing the XC functional leads to variations of the tilt angle within 2°. This highlights the stability of the deduced orientational parameter with respect to the computational method. On this basis and following the results of several works [14, 35–40] assessing vibrational properties obtained with DFT methods, it is concluded that the use of the B3LYP functional remains a reasonable choice for a combined description of the vibrational frequencies, normal modes, IR vectors and Raman tensors, since all these properties need to be predicted in a balanced way in order to properly simulate SFG spectra.

4. Conclusions

In this paper the normal coordinates, IR vectors and Raman tensors of the three methyl vibrations were investigated with DFT methods for different molecular systems with an increasingly long aliphatic chain. These data were then employed to simulate the SFG spectrum of a self-assembled monolayer of DDT on a platinum surface. This allowed the determination of the orientation of the terminal methyl group characterized by the tilt angle θ. The simulations on the 'frozen chain' models showed that the effect of the chain is rather modest with variations of the deduced tilt angle of about 2°. However, a more pronounced effect is observed for the 'frozen methyl' systems, which present variations of the tilt angle of about 6°, mostly due to the contribution of the methylene units localized next to the methyl group. Furthermore, the effects of the environment on the vibrational properties of DDT, as described by the PCM model, showed an almost negligible effect (less than 1°) on the tilt angle. Finally, the investigation of different XC functionals provided rather consistent results—with the exception of HSE06—with variations of the tilt angle within a 2° range.

More importantly, it is shown that the DFT calculations performed on the different models predict a tilt angle close to 45°, whereas a significantly smaller tilt angle of about 33° is deduced by using the analytical approach [8–10, 12], possibly due to the uncertainty on the depolarization ratio estimated for DDT. Since the analytical approach is less evolved than first principles calculations, it is concluded that DFT methodologies have to be preferred for the simulation of SFG spectra and for the deduction of orientational parameters.

References

[1] Kudelski A 2005 *Vib. Spectrosc.* **39** 200
[2] Schultz Z D and Levin I W 2011 *Annu. Rev. Anal. Chem.* **4** 343
[3] Trenary M 2000 *Annu. Rev. Phys. Chem.* **51** 381
[4] Tanaka M and Young R J 2006 *J. Mater. Sci.* **41** 963
[5] Shen Y R 2001 *Pure Appl. Chem.* **10** 1589
[6] Vidal F and Tadjeddine A 2005 *Rep. Prog. Phys.* **68** 1095
[7] Chen X, Clarke M L, Wang J and Chen Z 2005 *Int. J. Mod. Phys. B* **4** 691
[8] Hirose C, Akamatsu N and Domen K J 1992 *Appl. Spectrosc.* **46** 1051
[9] Hirose C, Akamatsu N and Domen K J 1992 *J. Chem. Phys.* **96** 997
[10] Hirose C, Yamamoto H, Akamatsu N and Domen K 1993 *J. Phys. Chem.* **97** 10064
[11] Guyot-Sionnest P, Hunt J H and Shen Y R 1987 *Phys. Rev. Lett.* **59** 1597
[12] Wang H-F, Gan W, Lu R, Rao Y and Wu B-H 2005 *Int. Rev. Phys. Chem.* **24** 191
[13] Mani A A, Schultz Z, Caudano Y, Champagne B, Humbert C, Dreesen L, Gewirth A, White J, Thiry P and Peremans A 2004 *J. Phys. Chem. B* **108** 16135
[14] Guthmuller J, Cecchet F, Lis D, Caudano Y, Mani A A, Thiry P A, Peremans A and Champagne B 2009 *ChemPhysChem* **10** 2132
[15] Morita A and Ishiyama T 2008 *Phys. Chem. Chem. Phys.* **10** 5801
[16] Gaigeot M P 2010 *Phys. Chem. Chem. Phys.* **12** 3336
[17] Ishiyama T and Morita A 2011 *J. Phys. Chem. C* **115** 13704
[18] Cecchet F, Lis D, Guthmuller J, Champagne B, Caudano Y, Silien C, Mani A A, Thiry P A and Peremans A 2010 *ChemPhysChem* **11** 607
[19] Armstrong J A, Bloembergen N, Ducuing J and Pershan P S 1962 *Phys. Rev.* **127** 1918
    Bloembergen N and Pershan P S 1962 *Phys. Rev.* **128** 606
[20] Shultz M J, Schnitzer C, Simonelli D and Baldelli S 2000 *Int. Rev. Phys. Chem.* **19** 123
    McCrea K and Somorjai G A 2000 *Adv. Catal.* **45** 385
    Richmond G L 2002 *Chem. Rev.* **102** 2693
    Vidal F and Tadjeddine A 2005 *Rep. Prog. Phys.* **68** 1095
    Shen Y R and Ostroverkhov V 2006 *Chem. Rev.* **106** 1140
    Gopalakrishnan S, Liu D, Allen H C, Kuo M and Shultz M J 2006 *Chem. Rev.* **106** 1155
[21] Shen Y R 1989 *Annu. Rev. Phys. Chem.* **40** 327
    Richmond G L, Robinson J M and Shannon V L 1988 *Prog. Surf. Sci.* **28** 1
    Shen Y R 1994 *Surf. Sci.* **299/300** 551
[22] Dreesen L, Humbert C, Celebi M, Lemaire J J, Mani A A, Thiry P A and Peremans A 2002 *Appl. Phys. B* **74** 621
[23] Epple M, Bittner A M, Kuhnke K, Kern K, Zheng W-Q and Abderrahmane T 2002 *Langmuir* **18** 773
[24] Yu Y, Lin K, Zhou X, Wang H, Liu S and Ma X 2007 *J. Raman Spectrosc.* **38** 1206
[25] Saito Y and Hamagouchi H 2001 *Chem. Phys. Lett.* **339** 351
[26] Lee C, Yang W and Parr R G 1998 *Phys. Rev. B* **37** 785
    Becke A D 1993 *J. Chem. Phys.* **98** 5648
[27] Frisch M J *et al* 2004 *Gaussian 03, Revision C.02* (Wallingford, CT: Gaussian)
[28] Frisch M J *et al* 2009 *Gaussian 09* (Wallingford, CT: Gaussian)
[29] Becke A D 1997 *J. Chem. Phys.* **107** 8554
[30] Hamprecht F A, Cohen A, Tozer D J and Handy N C 1998 *J. Chem. Phys.* **109** 6264
[31] Henderson T M, Izmaylov A F, Scalmani G and Scuseria G E 2009 *J. Chem. Phys.* **131** 044108
[32] Zhao Y and Truhlar D G 2007 *Theor. Chem. Acc.* **120** 215
[33] Yanai T, Tew D P and Handy N C 2004 *Chem. Phys. Lett.* **393** 51
[34] Merrick J P, Moran D and Radom L 2007 *J. Phys. Chem. A* **111** 11683
[35] Jiménez-Hoyos C A, Janesko B G and Scuseria G E 2008 *Phys. Chem. Chem. Phys.* **10** 6621
[36] Halls M D and Schlegel H B 1998 *J. Chem. Phys.* **109** 10587
[37] Halls M D and Schlegel H B 1999 *J. Chem. Phys.* **111** 8819
[38] Biczysko M, Panek P, Scalmani G, Bloino J and Barone V 2010 *J. Chem. Theor. Comput.* **6** 2115
[39] Zvereva E E, Shagidullin A R and Katsyuba S A 2011 *J. Phys. Chem. A* **155** 63
[40] Guthmuller J 2011 *J. Chem. Theor. Comput.* **7** 1082